Biotechnology Reports 32 (2021) e00682

Contents lists available at ScienceDirect

Biotechnology Reports

journal homepage: www.elsevier.com/locate/btre

Engineering a variant of IL-17RA with high binding affinity to IL-17A for optimized immunotherapy

Fatemeh Armaghan, Zahra Hajihassan *

Department of Life Science Engineering, Faculty of New Sciences and Technologies, University of Tehran, Tehran, Iran

ARTICLE INFO

Keywords:
IL-17A
Protein expression
E. coli
Immunotherapy

ABSTRACT

Immunotherapy is one of the most recently used treatments for numerous cancer types and also some autoimmune and inflammatory diseases. One of the valuable targets for immunotherapy is Interleukin-17A (IL-17A) or its receptor (IL-17RA) because overexpression of IL-17A as a pro-inflammatory cytokine is associated with several inflammatory, autoimmune and cancer diseases. In this study, the extracellular domain of IL-17RA involved in binding to IL-17A was mutated by using R software to achieve a variant with increased binding affinity to IL-17A. The ΔΔG value of –30.89 kcal/mol was calculated for the best variant (385) with point mutations of R265N, N91T, and W31K using the FoldX module. Also, the K_D for its interaction with IL-17A was calculated 0.06 nM by surface plasmon resonance (SPR) technique. Our results indicated that variant 385 could bind to IL-17A with higher binding affinity than wild-type one, so, it can be a good therapeutic candidate for blocking IL-17A.

1. Introduction

The interleukin-17 (IL-17) family consists of six members, IL-17A, IL-17B, IL-17C, IL-17D, IL-17E, and IL-17F, with different homologies and functions [1]. IL-17A has been known as a pro-inflammatory cytokine that is secreted mainly by activated CD4+ and CD8+ T cells, and also by a variety of adaptive and innate immune cells such as, γδ T cells, natural killer (NK) cells and natural killer T cells (NKT), and lymphoid tissue inducer (LTi) cells, and group 3 innate lymphoid cells (ILC3) [2]. IL-17A plays a key role in host defense against fungal and extracellular bacterial infections. On the other hand, overexpression of IL-17A increases the rate of growth, proliferation, maturation, angiogenesis, and most importantly, cell division and metastasis of cancer cells. Also, IL-17A induces inflammatory responses, and autoimmune diseases including rheumatoid arthritis and multiple sclerosis by binding to its receptor, and induction the expression of many mediators of inflammation [3].

There are different receptors for IL-17 family including IL-17RA, IL-17RB, IL-17RC, IL-17RD, and IL-17RE [4]. IL-17RA is the largest and well-known receptor in this family and also is more accessible than other receptors. Besides, the binding affinity of IL-17RA for IL-17A is higher than other receptors [5]. IL-17RA is a transmembrane protein with extracellular, transmembrane, and cytoplasmic regions. The major amino acids involved in the binding of IL-17RA to IL-17A are located at its extracellular domain [6]. As a result of this binding at the cell membrane surface, Nuclear Factor Kappa B (NF-κB), Mitogen-Activated Protein Kinase (MAPK) and the CCAAT/enhancer-binding protein (C/EBP) pathways are activated. Activation of these pathways leads to the induction of transcription and inflammatory factors expression [4]. Studies have shown that decreased levels of IL-17RA or IL-17A are associated with a reduction in tumor growth and inflammatory responses so, their blockade can play a crucial role in the treatment of inflammatory, autoimmune, and cancer diseases [7].

Today, various anti-IL-17A and anti-IL-17RA antibodies, known as Ixekizumab, Brodalumab, and Secukinumab, are used for the treatment of diseases related to this cytokine. These antibodies inhibit IL-17A activity by binding to IL-17A or its receptor. In spite of the therapeutic properties of the monoclonal antibodies, they also have side effects such as neutropenia, hypersensitivity reactions, nasopharyngitis, and upper respiratory tract infection. In addition, they cannot penetrate efficiently to the solid tumors because of their large size [8–11].

As the extracellular domain of IL-17RA is solely enough for binding to IL-17A, and most importantly, this binding does not activate intracellular signaling [6], so in this study, this domain was chosen as a receptor-like candidate and also a substitution for antibodies. In

* Corresponding author at: Department of Life Science Engineering, Faculty of New Sciences and Technologies, University of Tehran, North karegar street, Tehran, 1439957131, Iran.
E-mail address: hajihasan@ut.ac.ir (Z. Hajihassan).

https://doi.org/10.1016/j.btre.2021.e00682
Received 5 May 2021; Received in revised form 25 September 2021; Accepted 1 October 2021
Available online 28 October 2021

addition, some site-directed mutagenesis in this domain was performed to increase its binding affinity for IL-17A. Finally, this receptor-like protein was produced in *E. coli*, and its efficiency was investigated.

2. Materials and methods

Unless otherwise specified, all reagents were purchased from Merck Company (Germany).

2.1. Bioinformatics analysis

In this investigation, the extracellular domain of IL-17RA protein (E.D.IL-17RA) was selected and engineered to increase its binding affinity to the IL-17A. First, its sequence was extracted from the UniProt database (https://www.uniprot.org/) (Q96F46), and then binding sites between this domain and the IL-17A were identified by PDBsum database (www.ebi.ac.uk ⟩ Thornton-SRV ⟩ databases ⟩ pdbsum). Subsequently, by using Alanine scanning technique and ROBETTA server (http://robetta.bakerlab.org), essential amino acids and positions involved in the ligand and receptor interaction were identified. R software version 3.4.2 was used to create mutations at three positions of E.D.IL-17RA. In this mutagenesis, three amino acids in E.D.IL-17RA were replaced with ten amino acids with the ability of hydrogen or ionic bond formation. After constructing the protein library from these resulting 1000 protein mutants, each protein sequence was modeled by homology modeling with the Swiss model server (https://swissmodel.expasy.org/) and then minimized by Chimera software (version 1.12).

The complexes between E.D.IL-17RA mutants and IL-17A were created by Swiss PDB viewer server version 4.1 (https://spdbv.vital-it.ch). Finally, the binding energies between protein mutants and IL-17A were calculated using FoldX software (YASARA version 17.8.15). According to the measured binding energies, the best variant was selected; the best variant was the one whose binding energy had the most significant decrease over the rest of the mutants and also compared to the wild type.

Moreover, the protein-protein interactions of native IL-17RA and the selected mutant with IL-17A have been schematically presented by LigPlot v.2.2.4 [12].

2.2. Bacterial strain, expression vector, and culture conditions

The SHuffle (T7) strain of *E. coli* (Novagene-USA) was used as a host for protein expression. pET-21a (+) vector contained His-tag sequence, and the T7 promoter was purchased from Novagene (USA) for gene cloning. SHuffle T7 cells were grown at 28 °C and in Luria–Bertani (LB) medium (10 g/L tryptone, 5 g/L yeast extract, 10 g/L NaCl) (Sigma-USA) supplemented with 100 μg/ml Ampicillin and Streptomycin antibiotics (Sigma- USA) for selection of recombinant bacteria.

2.3. Construction of expression cassette

The codon-optimized cDNA of the best variant was synthesized by the ShineGene company (China). It was also cloned in pET-21a (+) expression vector using NdeI and XhoI restriction enzymes (Jena Bioscience-Germany) by the same company. The recombinant vector was subsequently transformed into SHuffle T7 competent cells by CaCl2 and heat shock procedure [13].

2.4. Protein expression

1% dilution of an overnight culture of SHuffle T7 cells transformed with a recombinant vector was transferred and grown in fresh LB medium at 28 °C until the absorbance at OD600nm reached 0.6. Protein expression was induced by addition of 1 mM IPTG (Sigma-USA). The cells were grown for about 16 h at 28 °C and were centrifuged at 4000 g for 20 min at 4 °C [14].

2.5. Protein extraction

To extract proteins, the cell pellet was suspended in 5 ml of lysis buffer (50 mM NaH2PO4, 300 mM NaCl, 10 mM imidazole, pH = 8.0). Then the sample was frozen in dry ice/ethanol and thaw in cold water. Sonication of the resultant suspension was done for 6 x (10 s on/ 10 s off) on ice, in order to fragment the cytoplasmic membrane. After centrifugation at 10,000 g for 30 min at 4 °C, the supernatant was saved on ice for further experiments [15].

2.6. SDS–PAGE and immunoblot analysis

Proteins were separated by 15% SDS–PAGE, according to Laemmli procedure under denaturing and reducing conditions [16]. For western blotting, the samples were run on SDS-PAGE and transferred onto a nitrocellulose membrane (Millipore-USA). The membrane subsequently was treated with anti-His His-tag monoclonal antibody (Sigma-USA) conjugated with horseradish peroxidase enzyme with 1:2000 dilution in PBS buffer containing 3% W/V skimmed milk. Detection of proteins was done using a solution of DAB (Biobasic-Canada) and hydrogen peroxide as enzyme substrates [17].

2.7. Protein purification

Extracted recombinant protein was purified easily by Ni^{+2}-NTA affinity chromatography (ABT-Spain) because produced protein has poly histidine tag on its C-terminal.

The column was pre-equilibrated with binding buffer (50 mM NaH2PO4, 300 mM NaCl, 10 mM imidazole, pH = 8). After loading the sample, and washing the column with washing buffer (50 mM NaH2PO4, 300 mM NaCl, 20 mM imidazole, pH = 8), elution buffer (50 mM NaH2PO4, 300 mM NaCl, 250 mM Imidazole, pH = 8) was added to the column to elute the target protein. The purified protein was then dialyzed against 10 mM Tris–HCl buffer (pH = 7.4) to remove imidazole. Protein purification was finally evaluated by SDS-PAGE method [18].

2.8. Protein concentration determination

In order to measure the concentration of purified protein, the Bradford method was used [19].

2.9. Circular dichroism (CD) spectroscopy

The secondary structure of the recombinant protein was determined using CD spectrophotometer (Aviv Model-215). The spectrum of purified protein in 10 mM Tris–HCl buffer pH = 7.4 was recorded in the range of 190–260 nm (Far-UV) with a spectral resolution of 1 nm. The scan speed was 20 nm/min, and the response time was 0.3330 s with a bandwidth of 1 nm. Quartz cell with a path length of 10 mm was used. Results were expressed as molar ellipticity [Θ], in deg × cm^2 × $dmol^{-1}$.

2.10. Surface plasmon resonance (SPR)

A two-channel cuvette-based SPR instrument with an incorporated auto sampler and an automatic flow injection system (Autolab ESPRIT, Metrohm Autolab, Utrecht, The Netherlands) was applied to measure and calculate the binding energy between IL-17A and the recombinant protein (the best variant of E.D.IL-17A). One channel was used to perform assay and the second channel was used to run reference measurements. Commercial sensing surfaces, the bare gold disks (BK7) coated with a 5 nm of titanium as an adhesion layer, and a sensing layer of 50 nm of gold, were supplied by Ssens bv, (The Netherlands). The outcome of the SPR measurements was automatically monitored using Data Acquisition software version 4.3.1 and all kinetic data were obtained using Kinetic Evaluation software version 5.4 (KE Instruments, The Netherlands).

Commercial recombinant IL-17A purchased from Bio Basic Inc. (Ontario, Canada) was immobilized on the sensor chip with the concentration of 50 μg/ml. The immobilization buffer used in this study was acetate buffer. pH of immobilization buffer is a critical factor that affects the interaction of IL-17A protein and the selected variant. pH should be adjusted about 0.5- to 1 unit lower than the pI (isoelectric point) of immobilized protein (IL-17A) [20]. As the pI of IL-17A is equal to 8.82, the immobilization buffer pH was chosen 7.82. For calculating the affinity constant between IL-17A and the selected variant, different concentrations of the latter (0.001, 0.01, 0.1, 1, 10, 100 nM) were used and the interaction between two proteins was conducted to assess the binding affinity and K_D measurement [21]. Also, for comparison, the same concentrations were used for the wild type receptor (IL-17RA) and its interaction with the ligand was investigated.

3. Results

3.1. Bioinformatics analysis

The complex structure extracted from the PDB database was given as an input to the PDBsum server to determine the binding sites between two proteins (IL-17A and IL-17RA); and the specific binding sites between two proteins were provided as output. As can be seen in Fig. 1, the interactions of these proteins are mostly composed of non-bonded (van der Waals) and hydrogen bonds.

To identify the most important binding sites of the complex, the three-dimensional structure of this complex extracted from the PDB database was provided as input for the ROBETTA server. According to the results of Alanine scanning technique, by replacing amino acids 26, 29, 93, 121, 123, 125, 146, 167, 216, 257, 258, 267 in the IL-17RA with alanine amino acid, the binding free energy changes became more negative (Table 1). This indicates that these 12 amino acids in the protein did not play an essential role in binding, and their replacement did not significantly affect the binding strength between these two proteins in the complex. However, with alanine substitution at positions 25, 27, 31, 32, 33, 86, 87, 88, 89, 90, 91, 92, 124, 127, 148, 176, 202, 204, 218, 251, 253, 255, 260, 261, 262, 264, 265, 266, the binding free energy between two proteins became more positive; it indicates decreasing the binding strength between these two proteins and the adverse effects of replacing the alanine with these amino acids. As a result, in recent cases an unstable complex will form. The most significant impact on the binding free energy between these two proteins occurred with mutations at the 31, 91, and 265 positions in IL-17RA; this indicated the importance of these amino acids in the binding energy between two proteins.

Afterward, the Ser, Thr, Tyr, Asn, Gln, Arg, Lys, His, Asp, Glu Glu-amino acids were selected to replace in the 31, 91, and 265 positions of IL-17RA because they have the ability to form hydrogen bonds. R software was used to perform these mutations. To do this, the protein sequence of E.D.IL-17RA extracted from the UniProt database, as well as a file containing the amino acids that form hydrogen bonds as input files were used for mutagenesis. The output of this software was a file

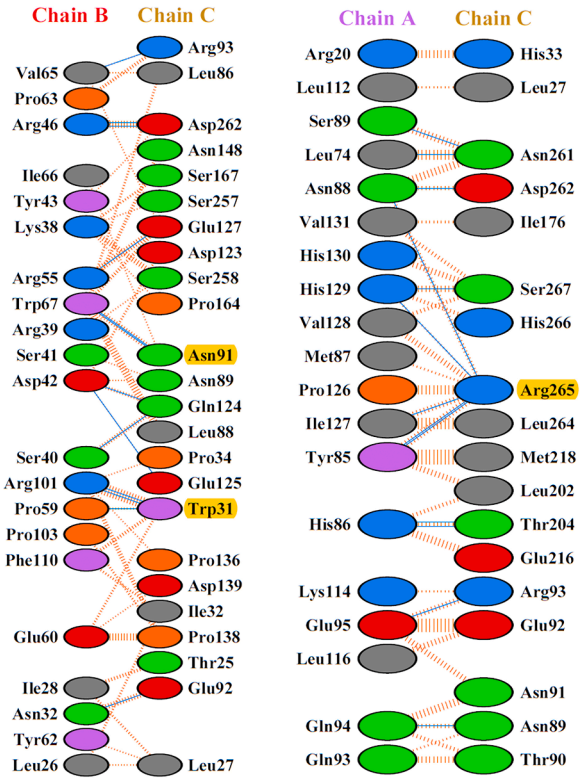

Fig. 1. Binding sites of IL-17A / IL-17RA complex determined by PDBsum server. Chain A and B belong to IL-17A and chain C belongs to IL-17RA. In this form, the orange bonds represent the van der Waals forces; the greater the number of atoms involved in this interaction, the larger the diameter of these orange bonds. Blue bonds represent hydrogen bonds. In this form, the amino acids involved in the interaction have been shown with different colors based on their physicochemical properties, such that the amino acids shown in red and blue are amino acids with negative and positive charge respectively and the amino acids shown in green are neutral. Aliphatic and aromatic amino acids are shown in gray and purple respectively. Proline is also shown in orange in this form.

Table 1
Alanine Scanning results indicating the effects of substitution of alanine residue in the binding sites of IL-17RA in the IL-17RA / IL-17A complex.

Amino acid number in chain C of IL-17RA protein	ΔΔG(kcal/mol) of IL-17RA/ IL-17A complex
25	0.68
26	−0.07
27	2.22
29	−0.19
31	5.79
32	0.84
33	0.33
86	0.83
87	0.06
88	1.42
89	1.15
90	0.04
91	2.37
92	0.66
93	−0.15
121	−0.17
123	−0.21
124	1.62
125	−0.17
127	0.90
146	−0.01
148	0.29
167	−0.17
176	0.32
202	1014
204	0.15
216	−0.19
218	0.50
251	1.57
253	0.13
255	0.51
257	−0.03
258	−0.10
259	0.00
260	0.04
261	2.24
262	1.01
264	1.17
265	5.36
266	0.34
267	−0.44

containing 1000 mutants of E.D.IL-17RA protein (see the additional file).

In order to make protein models, the Swiss model server was used. The Swiss model is a server for automated comparative modeling of protein three-dimensional (3D) structures. To do this, the sequence of mutant proteins was first given to this server, and then a template for modeling was introduced to it. In this study, the 3D structure of IL-17RA protein from the PDB database (3JVF) was introduced as a modeling template for this server.

Swiss-PdbViewer (aka DeepView) is as an application that provides a user-friendly interface allowing to analyze several proteins at the same time. In this study, it was used to construct protein complexes between the 3D structure of the IL-17A (4hr9), and all 1000 mutants of E.D.IL-17RA protein. FoldX is a software that predicts binding affinity changes and possible epistatic effects in protein complexes due to the multiple mutations. At this level, the protein complexes derived from Swiss-PdbViewer were introduced to FoldX to calculate the binding energy. Among the 1000 mutated sequences, twenty complexes had better binding energy than the wild type. Table 2 shows the binding energies of these complexes and amino acids at positions 31, 91, and 265, respectively. According to the table, the complex between mutant 385 and IL-17A had the best binding energy over other structures and the natural structure of IL-17RA. In this complex, lysine, threonine, and asparagine residues were placed respectively in positions 31, 91, and 265 instead of tryptophan, asparagine, and arginine. Table 3 shows many factors that were examined by Fold X software in the calculation of the binding energy between two proteins. The decreased binding energy in the complex of mutant 385 and IL-17A was due to electrostatic energy, Polar dissolution, van der Waals clashes, side-chain entropy, torsional clash and backbone clash created in the mutant complex.

In addition, the LigPlot program was used for more detailed analysis of the bonds, especially hydrogen bonds formed in the wild type IL-17RA and mutant 385. Although the amino acids Trp 31, Asn 91, Arg 265, which are mutated in variant 385, play an important role in the interaction of protein-protein in the native form, but the results showed that by replacing them, the number of hydrogen bonds increased. And this could be the important reason for decreased binding energy in the complex of mutant 385 and IL-17A. Fig. 2 shows that the number of hydrogen bonds in the wild type is 26, and by mutation, the number of hydrogen bonds has increased to 37.

Fig. 3 also shows the Qualitative Model Energy Analysis (QMEAN) factor for this variant equal to −2.29 obtained in Swiss model server. QMEAN is a scoring function based on geometric structure and estimates the score for a model both at the general level and at the regional level. It indicates the quality of the built model compared to the models that are laboratory-determined. If the value of this score is less than −4, it indicates a low-quality model. Global Model Quality Estimation (GMQE) is a quality estimation that combines properties from the target–template alignment and the template search method. The resulting GMQE score is expressed as a number between 0 and 1, reflecting the expected accuracy of a model built with that alignment and template and the coverage of the target. Larger numbers indicate higher reliability. GMQE value calculated for mutant 385 by the Swiss model server was 0.97. GMQE is a median of QMEAN and the number of beta carbon aberrations and intramolecular interactions, and the degree of solubility and angular torsion. The factors involved in GMQE were investigated individually, and all factors were of medium to high quality (Fig. 3).

Table 2
The binding energy of complexes between mutants of E.D.IL-17RA and IL-17A better than the wild type one calculated by FoldX software.

Mutant number	Position31	Position91	Position265	Binding energy (kcal/mol)
IL-17RA(wild type)	Trp	Asn	Arg	−23.69
M 385	Lys	Thr	Asn	−30.89
397 M	Lys	Tyr	Arg	−26.61-
819 M	Thr	Glu	Thr	−26.46
M 347	Lys	Asn	Arg	−26.09
M 657	Arg	Gln	Arg	−25.72
M 958	Tyr	Gln	Ser	−25.15
M 879	Thr	Ser	Thr	−24.82
M 348	Lys	Asn	Ser	−24.68
M 697	Arg	Tyr	Arg	−24.70
M 997	Tyr	Tyr	Arg	−24.50
M 757	Ser	Gln	Arg	−24.35
M 647	Arg	Asn	Arg	−24.34
M 949	Tyr	Asn	Thr	−24.3
M 877	Thr	Ser	Arg	−24.06
M 646	Arg	Asn	Gln	−23.89
M 844	Thr	Asn	Lys	−23.85
M 954	Tyr	Gln	Lys	−23.84
M 27	Asp	Glu	Arg	−23.75
M 775	Ser	Ser	Asn	−23.75
M 398	Lys	Tyr	Ser	−23.75

Table 3
Factors evaluated by Fold X software in the calculation of the binding energy.

Energy (kcal/mol)	Complex IL-17A/IL-17RA	Complex variant 385/IL-17A
Interaction Energy	−23.6978	−30.8863
Van der Waals	−37.2473	−34.0048
Electrostatics	−4.59057	−5.86532
Solvation Polar	53.3505	50.5623
Solvation Hydrophobic	−46.9037	−42.1107
Van der Waals clashes	10.9393	3.93548
Entropy sidechain	20.6412	21.3129
Entropy main chain	8.47832	8.29808
Torsional clash	1.02493	0.748188
Backbone clash	6.0954	5.05828
Entropy Complex	2.384	2.384
Energy ionisation	0.098062	0.101313

3.2. Protein expression and purification

Mutant 385 was considered as the best variant of E.D.IL-17RA, so its sequence was synthesized and cloned in pET-21a (+) vector, and then transformed to the Shuffle T7 strain. Protein expression was confirmed by SDS-PAGE and Western blotting techniques (Fig. 4). The appearance of the protein band on the nitrocellulose paper in western blotting indicates the reaction between the protein expressed (variant 385) containing the poly histidine-tag and anti-his-tag monoclonal antibody; it is a proof of protein expression. This protein was then successfully purified by Ni^{+2}–NTA chromatography. The 33-kDa band corresponding to variant 385 is visible in the Fig. 4a, indicating successful purification.

3.3. Structural analysis

In order to estimate the quality of the purified recombinant protein, the secondary structure of it after purification by Ni^{2+}-NTA chromatography was determined by CD spectroscopy. Furthermore, this structure was compared with the secondary structure of extracellular domain of native IL-17RA reported in the UniProt database (Q96F46) (Fig. 5). The percentage of secondary structure elements for purified protein was 17/3% α-Helix, 40% β-sheet, 20/8% β-turn, and 41% random coil, and in good consistency with the structure found in the UniProt (7.3% α-Helix, 44.1% β-sheet, 5.2% β-turn and 43.4% random coil). Comparison of numbers shows that due to the applied mutations in variant 385, the α-helix structure has changed more than β-sheet.

3.4. SPR characterization for interaction of variant 385 of E.D.IL-17RA with the immobilized IL-17A

The interaction of various concentrations of variant 385 with IL-17A was conducted to assess the binding affinity of two proteins and finally

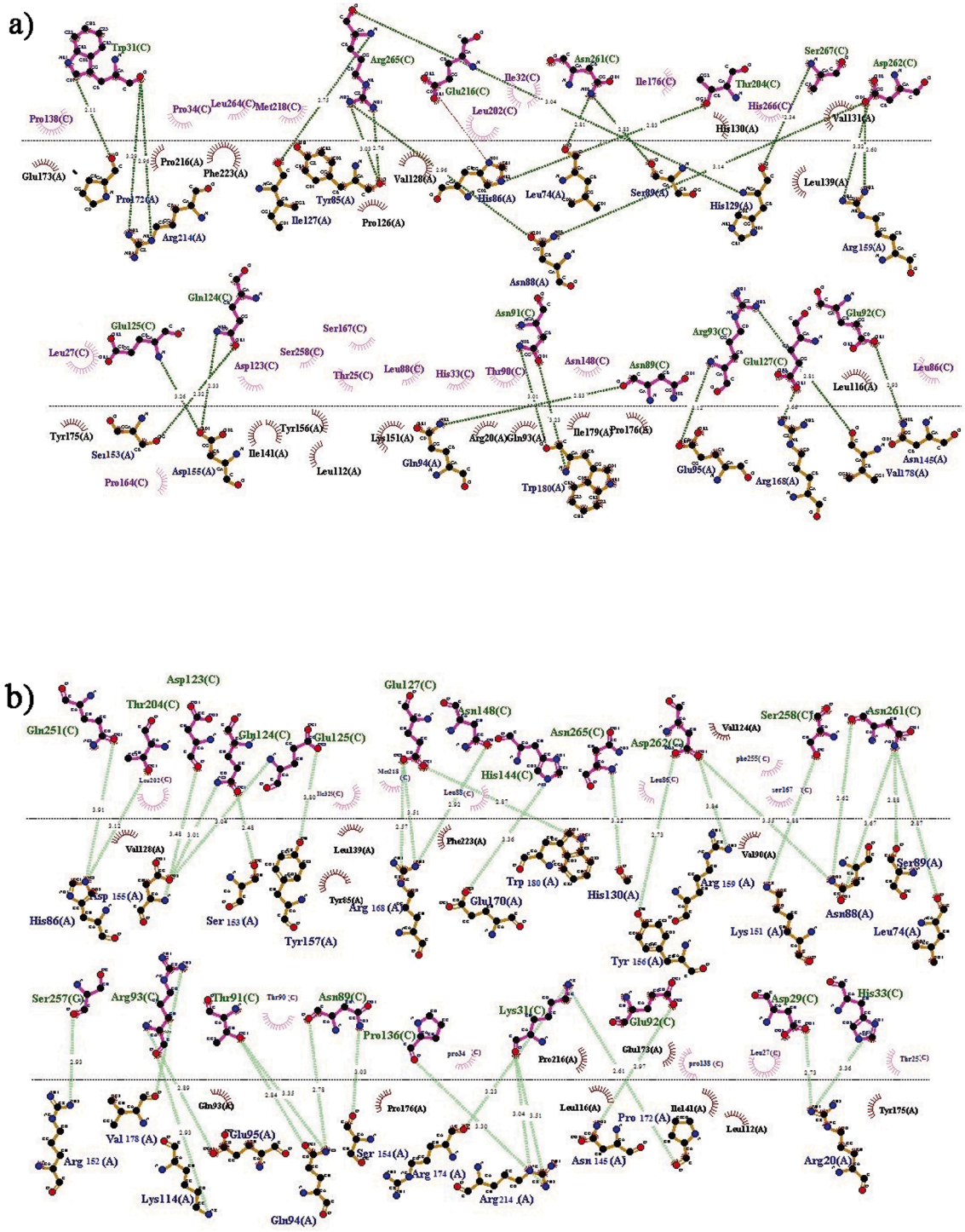

Fig. 2. The interactions at the protein–protein interface in (**a**) native form, and (**b**) variant 385 of E.D.IL-17RA with IL-17A obtained from the LigPlot program. Chain A belongs to IL-17A and chain C belongs to IL-17RA. Hydrogen bonds are indicated by green dotted lines. The amino acids involved in hydrophobic interactions are shown in purple and red.

the equilibrium dissociation constant (K_D) was measured [22]. Fig. 6 represents the stepwise immobilization of IL-17A on the chip; this process consists of 10 steps. These results indicated that IL-17A was successfully immobilized on the surface of the SPR chip.

As shown in Fig. 7a, the SPR sensorgram angle shifts are dependent on concentrations of variant 385 (from 0.001 to 100 nM). Using the "kinetic evaluation software ver.5.4″, K_D was determined 0.06 nM for binding of variant 385 to immobilized IL-17A. This low K_D value describes the interaction of this protein with the immobilized IL-17A with high affinity [23]. Also, K_D = 1.4 nM was calculated for interaction of wild type IL-17RA with IL-17A (Fig. 7b). Comparison of the K_D values showed that the binding affinity of the variant 385 increased for its ligand relative to the wild receptor.

4. Discussion

Immunotherapy is one of the most recently used treatments for numerous cancer types [24, 25]. Immune checkpoints as regulators of

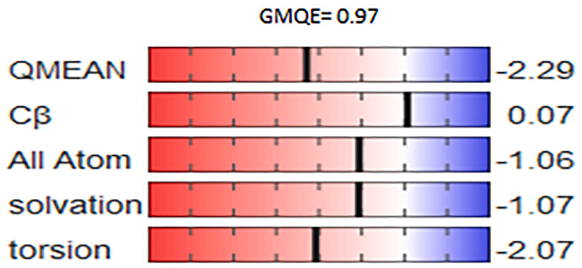

Fig. 3. The quality determinants of the model made using the homology modeling method. All factors are of medium to high quality.

the immune system have been valuable targets for cancer immunotherapy in recent years. Cytotoxic T lymphocyte antigen-4 or CTLA-4, programmed cell death protein-1 (PD-1) and programmed death-ligand 1 (PD-L1) are examples of these molecules [26]. Any drugs such as a monoclonal antibody or even a small protein or peptide that targets and blocks immune checkpoints can activate the immune system to kill cancer cells efficiently. For example, antibodies e.g. Pembrolizumab and Nivolumab, that bind to either PD-1 or PD-L1 and therefore block their interaction activate T cells and allow them to attack the tumors [27].

Nevertheless, despite many clinical applications of antibodies, in some cases they have serious side effects such as neutropenia,

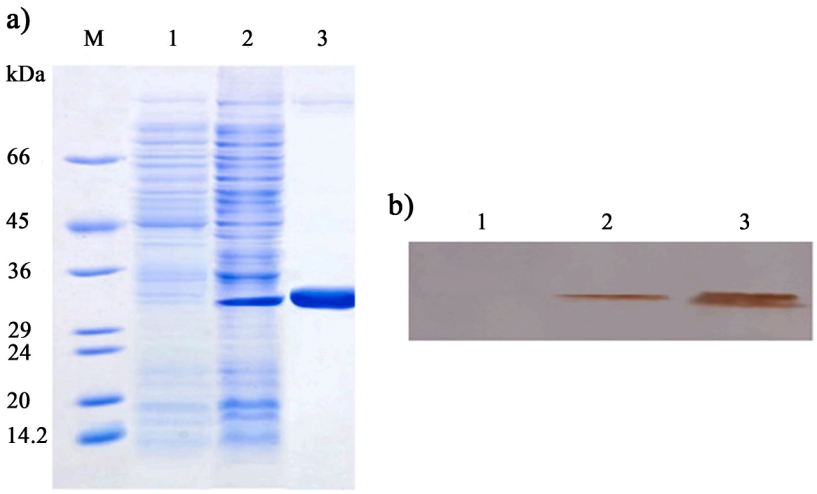

Fig. 4. Expression analysis of variant 385 extracted from recombinant SHuffle T7 strain by 15% SDS gel electrophoresis (a) and Western blotting (b) respectively. All experiments were repeated three times under identical experimental conditions. Lanes 1, 2 and 3 are respectively negative control (proteins extracted from SHuffle T7 lacking recombinant pET21a vector), cytoplasmic proteins extracted from recombinant bacteria and purified variant 385 after purification by Ni^{+2}–NTA chromatography. M shows the molecular weight marker.

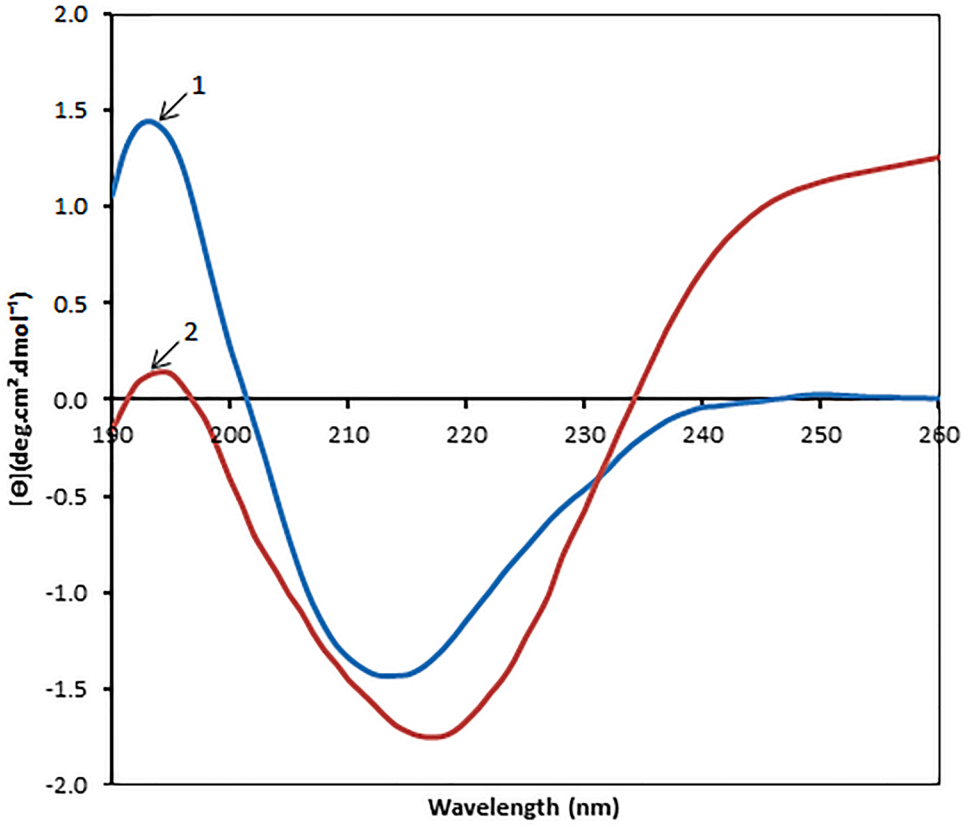

Fig. 5. Far UV CD spectra of wild type E.D.IL-17RA (1) and variant 385 of it (2). Each spectrum was obtained at 25 °C with a 10 mm path length cell.

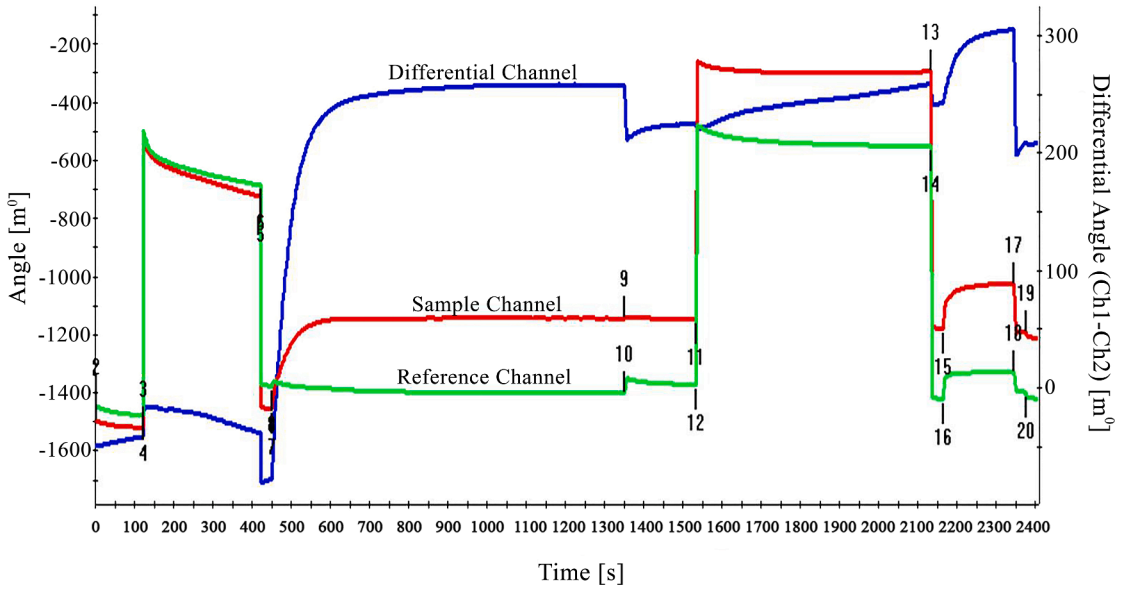

Fig. 6. Sensorgram showing different steps [(1,2) baseline, (3,4) EDC—NHS activation, (5,6) washing, (7,8) IL-17A coupling, (9,10) washing, (11,12) deactivation, (13,14) washing, (15,16) regeneration, (17,18) washing, and (19,20) back to baseline] involved in the immobilization of 50 μg/mL IL-17A on gold chip.

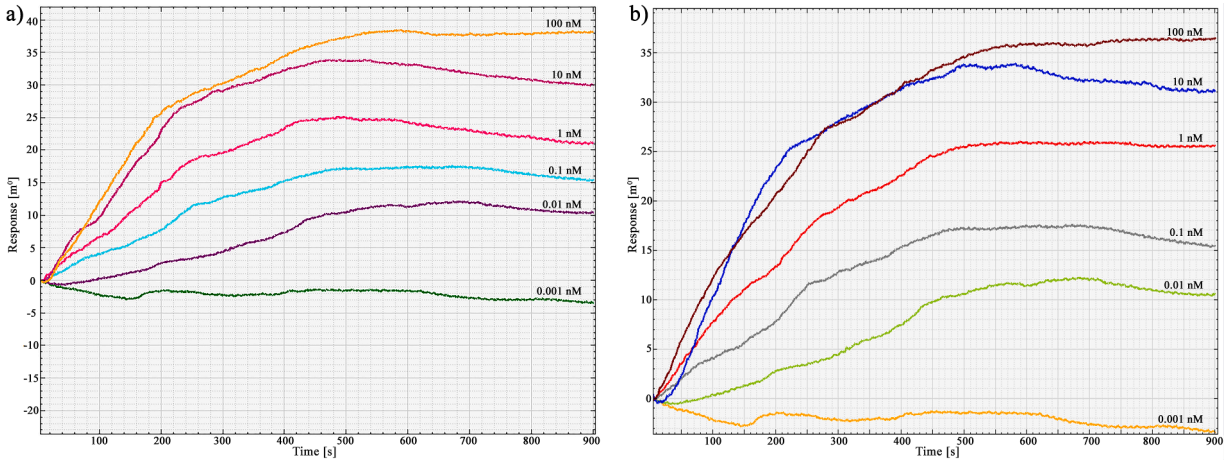

Fig. 7. Overlay plot for the interaction of different concentrations (0.001, 0.01, 0.1, 1, 10, 100 nM) of variant 385 of E.D.IL-17RA (a), and wild-type IL-17RA (b) with 50 μg/mL immobilized IL-17A.

hypersensitivity reactions, nasopharyngitis, and upper respiratory tract infection. The second problem is the time-consuming and costly process of producing these therapeutic proteins [28]. Furthermore, using antibodies has limitations that can reduce their effectiveness, such as their limited tissue/tumor penetration due to their large size [29]. An important weakness reported for some immunotherapeutic antibodies is related to their Fc-effector functions. Although this Fc-mediated effect is required for the efficacy of some antibodies, but in treatment with antibodies targeting CTLA-4 or PD-1 and PD-L1, the number of circulating T-cells decreased because of unwanted function of Fc in undesirable depletion of the T cells [30, 31].

Due to the disadvantages mentioned for antibodies, scientists have turned their attention to the production of small peptide or protein molecules instead of large antibodies. An example of these therapeutic small proteins is the high-affinity consensus PD-1(HAC-PD1) protein, a variant of the PD-1, reported by Maute and his colleagues in 2015. It binds to PD-L1 like antibodies but it does not have inherent limitations of antibodies. In addition, it has enhanced penetration to tumors because of its small size [32].

Immunotherapy and especially monoclonal antibodies have also been used to treat autoimmune and inflammation diseases; for instance, antibodies such as Infliximab and Adalimumab as inhibitors of Tumor necrosis factor-α (TNF-α) are used to treat rheumatoid arthritis [33]. IL-17A or its receptor, IL-17RA, can be another candidate for immunotherapy, because studies have shown that overexpression of it is associated with inflammatory and autoimmune diseases, and cancer progression too. To date, many monoclonal antibodies have been approved for use in treating diseases related to this cytokine [8]. Because of side effects and limitations mentioned for antibodies, in this study a variant of IL-17RA with high binding affinity for IL-17A was designed. IL-17RA is a well-known receptor for IL-17A and has extracellular, transmembrane, and cytoplasmic regions. Furthermore, studies have shown that only the extracellular domain of the receptor is sufficient for binding (6); so, only the sequence of this domain was selected and mutated in three positions with crucial role in binding. By using the R software these three amino acids, R265, N91, W31, were mutated with ten other amino acids with the ability to form ionic or hydrogen bonds because they are stronger bonds than hydrophobic and van der Waals forces. The bioinformatics results showed that the mutant 385 was the best variant with point mutations R265N, N91T, W31K and higher

binding energy compared to the wild type IL-17RA so, it can compete with IL-17RA for binding to the IL-17A. The extra cellular domain of IL-17RA used in this study is glycosylated but according to the literature, glycosylation is not necessary for the function of this protein, so this variant was expressed in the SHuffle (T7) strain of *E. coli*[6].

Also, since the function of proteins is affected by their correct structure, the secondary structure of this variant was determined by CD spectroscopy; the percentage of secondary structure elements for it were 17/3% α-Helix, 40% β-sheet, 20/8% β-turn, and 41% random coil. Comparing with secondary structure of extracellular domain of wild type IL-17RA reported in UniProt (Q96F46) showed acceptable similarity especially in β-sheet structure.

Interaction of recombinant variant 385 with IL-17A was studied also experimentally using SPR technique. For this interaction low K_D value (0.06 nM) was obtained confirming higher binding affinity for IL-17A than wild type IL-17RA with $K_D = 1.4$ nM. According to the results obtained in several articles in this field, this low value for K_D indicates a very high binding affinity for IL-17A because if K_D is $\leq$ 10 nM, it indicates high affinity interactions [34, 35].

5. Conclusions

These results, overally indicated that variant 385 of E.D.IL-17RA with point mutations of W31K, N91T and R265N could bind to IL-17A with high affinity. Therefore, it can be a good therapeutic candidate for blocking IL-17A to control or prevent the progression of autoimmune, inflammatory, and cancer diseases.

6. Author contributions

Z.H. designed the experiments and interpreted data. F.A. performed the experiments. Both authors wrote the manuscript and approved the final version of it.

CRediT authorship contribution statement

Fatemeh Armaghan: Investigation, Writing – original draft. **Zahra Hajihassan:** Formal analysis, Funding acquisition, Project administration, Writing – review & editing.

Declaration of Competing Interest

The authors declare that they have no conflict of interest.

Acknowledgement

The authors would like to acknowledge the financial support of University of Tehran and University of Tehran Science & Technology Park under Grant Numbers 28669/06/13 and 120076 respectively for this research. We also thank Dr. Nasser Ansaripour for his help in using bioinformatics tools.

Supplementary materials

Supplementary material associated with this article can be found, in the online version, at doi:10.1016/j.btre.2021.e00682.

References

[1] T. Moseley, D.R. Haudenschild, L. Rose, A.H. Reddi, Interleukin-17 family and IL-17 receptors, Cytokine Growth Factor Rev. 14 (2003) 155–174.
[2] Y. Iwakura, H. Ishigame, S. Saijo, S. Nakae, Functional specialization of interleukin-17 family members, Immunity 34 (2011) 149–162.
[3] J. Witowski, K. Książek, A. Jörres, Interleukin-17: a mediator of inflammatory responses, Cell. Mol. Life Sci. 61 (2004) 567–579.
[4] L. Sarah, S. Gaffen, Structure and signaling in the IL-17 receptor superfamily, Nat. Rev. Immunol. 9 (2009) 556–571.
[5] L.K. Ely, S. Fischer, K.C. Garcia, Structural basis of receptor sharing by interleukin 17 cytokines, Nat. Immunol. 10 (2009) 1245.
[6] S. Liu, X. Song, B.A. Chrunyk, S. Shanker, L.R. Hoth, E.S. Marr, M.C. Griffor, Crystal structures of interleukin 17A and its complex with IL-17 receptor A, Nat. Commun. 4 (2013) 1888.
[7] A. Beringer, M. Noack, P. Miossec, IL-17 in chronic inflammation: from discovery to targeting, Trends Mol. Med. 22 (2016) 230–241.
[8] J. Bilal, A. Berlinberg, S. Bhattacharjee, J. Trost, I.B. Riaz, D.J. Kurtzman, A systematic review and meta-analysis of the efficacy and safety of the interleukin (IL)-12/23 and IL-17 inhibitors ustekinumab, secukinumab, ixekizumab, brodalumab, guselkumab and tildrakizumab for the treatment of moderate to severe plaque psoriasis, Journal of Dermatological Treatment 29 (2018) 569–578.
[9] C.V. Preuss, J. Quick, Ixekizumab, StatPearls (2020) [Internet].
[10] N.M. Golbari, B.M. Basehore, P.M. Zito, Brodalumab (2019).
[11] M. Sanford, K. McKeage, Secukinumab: first global approval, Drugs 75 (2015) 329–338.
[12] A.C. Wallace, R.A. Laskowski, J.M. Thornton, LIGPLOT: a program to generate schematic diagrams of protein-ligand interactions, Protein Eng. Des. Sel. 8 (1995) 127–134.
[13] J. Sambrook, D.W. Russell, Molecular cloning: a Laboratory Manual, Cold Spring Harbor Laboratory Press, Cold Spring Harbor, N.Y., 2001.
[14] J. Lobstein, C.A. Emrich, C. Jeans, M. Faulkner, P. Riggs, M. Berkmen, SHuffle, a novel Escherichia coli protein expression strain capable of correctly folding disulfide bonded proteins in its cytoplasm, Microb. Cell Fact. 11 (2012) 753.
[15] A. QIAexpressionist, A handbook for high-level expression and purification of 6xhis-tagged proteins, Qiagen (2002) p1–125.
[16] U.K. Laemmli, Cleavage of structural proteins during the assembly of the head of bacteriophage T4, Nature 227 (1970) 680–685.
[17] A. Demaio, Protein Blotting and Immunoblotting Using Nitrocellulose membranes, Protein blotting, Oxford University Press, Oxford, 1996, pp. 11–32.
[18] Z. Hajihassan, M. Abdi, E. Roshani Yasaghi, A. Rabbani-Chadegani, Optimization of recombinant beta-NGF purification using immobilized metal affinity chromatography, Minerva Biotecnol. 29 (2017) 126–132.
[19] M.M. Bradford, A rapid and sensitive method for the quantitation of microgram quantities of protein utilizing the principle of protein-dye binding, Anal. Biochem. 72 (1976) 248–254.
[20] L. Jason-Moller, M. Murphy, J. Bruno, Overview of Biacore systems and their applications, Curr. Protoc. Protein Sci. 45 (2006), 19.13. 11-19.13. 14.
[21] R.A. Taheri, A.H. Rezayan, F. Rahimi, J. Mohammadnejad, M. Kamali, Evaluating the potential of an antibody against recombinant OmpW antigen in detection of Vibrio cholerae by surface plasmon resonance (SPR) biosensor, Plasmonics 12 (2017) 1493–1504.
[22] H.H. Nguyen, J. Park, S. Kang, M. Kim, Surface plasmon resonance: a versatile technique for biosensor applications, Sensors 15 (2015) 10481–10510.
[23] B. Sikarwar, P.K. Sharma, A. Srivastava, G.S. Agarwal, M. Boopathi, B. Singh, Y. K. Jaiswal, Surface plasmon resonance characterization of monoclonal and polyclonal antibodies of malaria for biosensor applications, Biosens. Bioelectron. 60 (2014) 201–209.
[24] C.R. Lichtenstern, R.K. Ngu, S. Shalapour, M. Karin, Immunotherapy, inflammation and colorectal cancer, Cells 9 (2020) 618.
[25] D.A. Boardman, M.K. Levings, Cancer immunotherapies repurposed for use in autoimmunity, Nat. Biomed. Eng. 3 (2019) 259–263.
[26] P. Sharma, J.P. Allison, Immune checkpoint targeting in cancer therapy: toward combination strategies with curative potential, Cell 161 (2015) 205–214.
[27] H.O. Alsaab, S. Sau, R. Alzhrani, K. Tatiparti, K. Bhise, S.K. Kashaw, A.K. Iyer, PD-1 and PD-L1 checkpoint signaling inhibition for cancer immunotherapy: mechanism, combinations, and clinical outcome, Front. Pharmacol. 8 (2017) 561.
[28] I. Mellman, G. Coukos, G. Dranoff, Cancer immunotherapy comes of age, Nature 480 (2011) 480–489.
[29] C.M. Lee, I.F. Tannock, The distribution of the therapeutic monoclonal antibodies cetuximab and trastuzumab within solid tumors, BMC Cancer 10 (2010) 255.
[30] T.R. Simpson, F. Li, W. Montalvo-Ortiz, M.A. Sepulveda, K. Bergerhoff, F. Arce, C. Roddie, J.Y. Henry, H. Yagita, J.D. Wolchok, Fc-dependent depletion of tumor-infiltrating regulatory T cells co-defines the efficacy of anti–CTLA-4 therapy against melanoma, J. Exp. Med. 210 (2013) 1695–1710.
[31] J.R. Brahmer, C.G. Drake, I. Wollner, J.D. Powderly, J. Picus, W.H. Sharfman, E. Stankevich, A. Pons, T.M. Salay, T.L. McMiller, Phase I study of single-agent anti–programmed death-1 (MDX-1106) in refractory solid tumors: safety, clinical activity, pharmacodynamics, and immunologic correlates, J. Clin. Oncol. 28 (2010) 3167.
[32] R.L. Maute, S.R. Gordon, A.T. Mayer, M.N. McCracken, A. Natarajan, N.G. Ring, R. Kimura, J.M. Tsai, A. Manglik, A.C. Kruse, Engineering high-affinity PD-1 variants for optimized immunotherapy and immuno-PET imaging, Proc. Natl. Acad. Sci. 112 (2015). E6506-E6514.
[33] F.M. Meier, M. Frerix, W. Hermann, U. Muller-Ladner, Current immunotherapy in rheumatoid arthritis, Immunotherapy 5 (9) (2013) 955–974.
[34] D. Wassaf, G. Kuang, K. Kopacz, Q.-.L. Wu, Q. Nguyen, M. Toews, J. Cosic, J. Jacques, S. Wiltshire, J. Lambert, High-throughput affinity ranking of antibodies using surface plasmon resonance microarrays, Anal. Biochem. 351 (2006) 241–253.
[35] A.C. Roque, C.S. Silva, M.Â. Taipa, Affinity-based methodologies and ligands for antibody purification: advances and perspectives, J. Chromatogr. A 1160 (2007) 44–55.